Electrochemical Reduction of CO_2 to CO Catalyzed by a Bimetallic Palladium Complex

James W. Raebiger,[†] Jeffrey W. Turner,[†] Bruce C. Noll,[‡] Calvin J. Curtis,[†] Alex Miedaner,[†] Brian Cox,[†] and Daniel L. DuBois*[,†,§]

National Renewable Energy Laboratory, 1617 Cole Boulevard, Golden, Colorado 80401, and Department of Chemistry and Biochemistry, University of Notre Dame, 251 Nieuwland Science Hall, Notre Dame, Indiana 46556-5670

Received March 12, 2006

The bis(triphosphine) ligand $C_6H_4\{P[CH_2CH_2P(C_6H_{11})_2]_2\}_2$, *m*-(triphos)$_2$ (**1**), is synthesized by the reaction of *m*-bis(phosphino)benzene with 4 equiv of vinyldicyclohexylphosphine. Reaction of **1** with 2 equiv of $[Pd(CH_3CN)_4](BF_4)_2$ results in the formation of the bimetallic complex $\{m\text{-(triphos)}_2\text{-}[Pd(CH_3CN)]_2\}(BF_4)_4$ (**2**). A structural study of **2** confirms the presence of two [Pd(triphosphine)-$(CH_3CN)]^{2+}$ substituents at the meta positions of a benzene ring. Complex **2** catalyzes the electrochemical reduction of CO_2 to CO in acidic dimethylformamide solutions. The kinetics of this reaction have been studied, and the reaction is 0.5 order in catalyst and first order in CO_2. This catalyst exhibits catalytic rates comparable to that of its monometallic analogues. Significantly higher turnover numbers are observed for **2** than observed previously for monometallic, bimetallic, and dendritic complexes of this class of catalysts.

Introduction

Electrochemical concentration and reduction of CO_2 provides a potential renewable route to carbon-based fuels and chemicals in addition to biomass. Recently, electrochemical separation and pumping of CO_2 from 0.5% CO_2 feed streams to nearly 100% CO_2 in the exit gas streams have been reported for a single pumping cycle.[1] In addition, numerous homogeneous and heterogeneous catalysts have been reported for electrochemical CO_2 reduction. The products observed in these various catalytic reductions include oxalate, carbon monoxide, formate, carboxylic acids, formaldehyde, acetone, methanol, methane, and ethylene. They represent reductions by one,[2] two,[3,4] four,[5] six,[6] and eight,[7] electrons per carbon atom. The electrochemical reductions of CO_2 to methane and ethylene at copper electrodes are examples of extremely complex reactions that can occur at electrode surfaces.[7] However, these reactions require large overpotentials, and consequently they are not energy efficient.

Typically homogeneous complexes and enzymes catalyze two-electron reductions of CO_2 to formate or CO,[3] although four- and six-electron reductions have also been reported.[5,6] Our laboratory has developed and studied the use of [Pd(triphosphine)-$(CH_3CN)]^{2+}$ complexes as catalysts for the electrochemical

* To whom correspondence should be addressed. E-mail: daniel.dubois@pnl.gov.

[†] National Renewable Energy Laboratory.

[‡] University of Notre Dame.

[§] Current address: Chemical Sciences Division, Pacific Northwest National Laboratory, Richland, WA 99352.

(1) (a) Scovazzo, P.; Poshusta, J.; DuBois, D. L.; Koval, C. A.; Noble, R. D. *J. Electrochem. Soc.* **2003**, *150*, D91−D98. (b) DuBois, D. L.; Miedaner, A.; Bell, W.; Smart, J. C. In *Electrochemical and Electrocatalytic Reactions of Carbon Dioxide*; Sullivan, B. P., Krist, K., Guard, H. E., Eds.; Elsevier: New York, 1993; Chapter 4.

(2) (a) Meshitsuka, S.; Ichikawa, M.; Tamaru, K. *J. Chem. Soc., Chem. Commun.* **1974**, 158−159. (b) Eggins, B. R.; Bennett, E. M.; McMullan, E. A. *J. Electroanal. Chem.* **1996**, *408*, 165−171. (c) Eggins, B. R.; Ennis, C.; McConnell, R.; Spence, M. *J. Appl. Electrochem.* **1997**, *27*, 706−712. (d) Becker, J. Y.; Vainas, B.; Eger, R.; Kaufman, L. *J. Chem. Soc., Chem. Commun.* **1985**, 1471−1472. (e) Rudolph, M.; Dautz, S.; Jäger, E. G. *J. Am. Chem. Soc.* **2000**, *122*, 10821−10830. (f) Gennaro, A.; Isse, A. A.; Savéant, J. M.; Severin, M. G.; Vianello, E. *J. Am. Chem. Soc.* **1996**, *118*, 7190−7196.

(3) (a) Fisher, B.; Eisenberg, R. *J. Am. Chem. Soc.* **1980**, *102*, 7363−7365. (b) Bhugun, I.; Lexa, D.; Savéant, J. M. *J. Am. Chem. Soc.* **1994**, *116*, 5015−5016. (c) Bhugun, I. D.; Lexa, D.; Savéant, J. M. *J. Am. Chem. Soc.* **1996**, *118*, 1769−1776. (d) Dhanasekaran, T.; Grodkowski, J.; Neta, P.; Hambright, P.; Fujita, E. *J. Phys. Chem. A* **1999**, *103*, 7742−7748. (e) Grodkowski, J.; Neta, P.; Fujita, E.; Mahammed, A.; Simkhovich, L.; Gross, Z. *J. Phys. Chem. A* **2002**, *106*, 4772−4778. (f) Ogata, T.; Yanagida, S.; Brunschwig, B. S.; Fujita, E. *J. Am. Chem. Soc.* **1995**, *117*, 6708−6716. (g) Isse, A. A.; Gennaro, A.; Vianello, E. *J. Mol. Cat.* **1991**, *70*, 197−208. (h) Pearce, D. J.; Pletcher, D. *J. Electroanal. Chem.* **1986**, *197*, 317−330. (i) Beley, M.; Collin, J. P. Ruppert, R.; Sauvage, J. P. *J. Am. Chem. Soc.* **1986**, *108*, 7461−7467. (j) Hawecker, J.; Lehn, J. M.; Ziessel, R. *Helv. Chim. Acta* **1986**, *69*, 1990−2012. (k) Stor, G. J.; van Outersterp, J. W. M.; Stufke, D. J. *Organometallics* **1995**, *14*, 1115−1131. (l) Christensen, P.; Hamnett, A.; Muir, A. V. G.; Timney J. A. *J. Chem. Soc., Dalton Trans.* **1992**, 1455−1463. (m) Johnson, F. P. A.; George, M. W.; Hartl, F.; Turner, J. J. *Organometallics* **1996**, *15*, 3374−3387. (n) Sullivan, B. P.; Bolinger, C. M.; Conrad, D.; Vining, W. J.; Meyer, T. J. *J. Chem. Soc., Chem. Commun.* **1985**, 1414−1416. (o) Gibson, D. H.; Yin, X.; He, H. Y.; Mashuta, M. S. *Organometallics* **2003**, *22*, 337−346. (p) Isse, A. A.; Gennaro, A.; Vianello, E.; Floriani, C. *J. Mol. Catal.* **1991**, *70*, 197−208. (q) Fujihira, M.; Hirata, Y.; Suga, K. *J. Electroanal. Chem.* **1990**, *292*, 199−215. (r) Lieber, C. M.; Lewis, N. S. *J. Am. Chem. Soc.* **1984**, *106*, 5033−5034. (s) Atoguchi, T.; Aramata, A.; Kazusaka, A.; Enyo, M. *J. Electroanal. Chem.* **1991**, *318*, 309−320. (t) Furuya, N.; Matsui, K. *J. Electroanal. Chem.* **1989**, *271*, 181−191. (u) Chardon-Noblat, S.; Deronzier, A.; Ziessel, R.; Zsoldos, D. *Inorg. Chem.* **1997**, *36*, 5384−5389. (v) Arana, C.; Yan, S.; Keshavarz-K, M.; Potts, K. T.; Abruña, H. D. *Inorg. Chem.* **1992**, *31*, 3680−3682. (w) Pugh, J. R.; Bruce, M. R. M.; Sullivan, B. P.; Meyer, T. J. *Inorg. Chem.* **1991**, *30*, 86−91. (x) Komeda, N.; Nagao, H.; Matsui, T.; Adachi, G.; Tanaka, K. *J. Am. Chem. Soc.* **1992**, *114*, 3625−3630. (y) Parkinson, B.; Weaver, P. *Nature* **1984**, *309*, 148−149.

(4) (a) Bringmann, J.; Dinjus, E. *Appl. Organomet. Chem.* **2001**, *15*, 135−140. (b) Amatore, C.; Jutand, A.; Khalil, F.; Nielsen, M. F. *J. Am. Chem. Soc.* **1992**, *114*, 7076−7085. (c) Amatore, C.; Jutand, A. *J. Am. Chem. Soc.* **1991**, *113*, 2819−2825. (d) Fauvarque, J. F.; Chevrot, C.; Jutand, A.; Francois, M.; Perichon, J. *J. Organomet. Chem.* **1984**, *264*, 273−281. (e) Dérien, S.; Duñach,; E.; Périchon, J. *J. Am. Chem. Soc.* **1991**, *113*, 8447−8454.

(5) (a) Sende, J. A. R.; Arana, C. R.; Hernández, L.; Potts, K. T.; Keshevarz-K, M.; Abruna, H. D. *Inorg. Chem.* **1995**, *34*, 3339−3348. (b) Mizukawa, T.; Tsuge, K.; Nakajima, H.; Tanaka, K. *Angew. Chem., Int. Ed.* **1999**, *38*, 362−363. (c) Nakajima, H.; Kushi, Y.; Nagao, H.; Tanaka, K. *Organometallics* **1995**, *14*, 5093−5098.

10.1021/om060228g CCC: $33.50
Publication on Web 06/02/2006

reduction of CO_2 to CO.[8−11] These catalysts exhibit high catalytic rates (10−300 M^{-1} s^{-1}), high selectivities (>90%), and low overpotentials (100−300 mV). Even higher catalytic rates (> 10^4 M^{-1} s^{-1}) were obtained using bimetallic palladium complexes in which two triphosphine units were bridged by a methylene group.[12] However, turnover numbers for these monometallic and bimetallic catalysts have been low, typically 10−100 for the production of CO. In this paper, we describe efforts to develop bimetallic palladium complexes with greater stability.

Experimental Section

General Comments. All reactions were carried out under a nitrogen atmosphere using standard Schlenk techniques. Dichloromethane and acetonitrile were distilled from calcium hydride under nitrogen. Dimethylformamide (Burdick and Jackson) was stored under nitrogen. ^1H and $^{31}P\{^1H\}$ NMR spectra were recorded on a Varian Unity 300 MHz spectrometer at 299.75 and 121.42 MHz, respectively. ^1H chemical shifts are reported relative to tetramethylsilane using residual solvent protons as a secondary reference. ^{31}P chemical shifts are reported relative to external phosphoric acid. Elemental analyses were performed by Galbraith Laboratories, Inc. $[Pd(NCCH_3)_4](BF_4)_2$,[14] *m*-bis(diphosphino)benzene,[15,16] and vinyldicyclohexylphosphine[17] were prepared using literature procedures.

Syntheses. $C_6H_4\{P[CH_2CH_2P(C_6H_{11})_2]_2\}_2$, *m*-(triphos)$_2$ (1). A sealed Schlenk flask containing a mixture of 1,3-bis(phosphino)-benzene (0.50 g, 0.0035 mol), vinyldicyclohexylphosphine (3.35 g, 0.015 mol), and 2,2′-azobis(2-methylproprionitrile) (AIBN, 0.1 g) was placed inside a Rayonet photoreactor and irradiated at 254 nm for 3 h. The product was heated to 100 °C for 3 h in a dynamic vacuum to remove volatile naterials. After cooling, the resulting white solid (3.50 g, 96%) was recrystallized from dichloromethane/ethanol in approximately 70% yield. $^{31}P\{^1H\}$ NMR (toluene-d_8): 1.55 ppm (d, $^3J_{PP}$ = 25 Hz, PCy_2), −14.38 ppm (t, C_6H_4P). ^1H NMR (toluene-d_8): 8.03 ppm (t, 6.9 Hz, Ar-*H*); 7.50 ppm (t, 6.0 Hz, Ar-*H*); 7.17 ppm (t, 7.5 Hz, Ar-*H*); 1.1−2.2 ppm (m's, cyclohexyl and methylene protons).

{*m*-(triphos)$_2$[Pd(CH$_3$CN)]$_2$}(BF$_4$)$_4$ (2). A solution of $[Pd(CH_3CN)_4](BF_4)_2$ (0.45 g, 0.001 mol) in acetonitrile (30 mL) was added to a solution of **1** in toluene (1.65 mL of a 0.3 M stock solution, 0.0005 mol), and the resulting solution was stirred at room temperature overnight. Removal of the solvent with a vacuum yielded a yellow powder (0.80 g, 95%). This product is pure by NMR spectroscopy. It can be recrystallized from a mixture of dichloromethane and ethanol. Anal. Calcd for $C_{66}H_{114}B_4F_{16}N_2P_6Pd_2$: C, 47.14; H, 6.83. Found: C, 46.69; H, 6.92. $^{31}P\{^1H\}$ NMR (CD_3CN): 119.4 ppm (t, $^3J_{PP}$ = 4 Hz, C_6H_4P), 76.6 ppm (d, PCy_2). ^1H NMR (CD_3CN): 7.7−8.2 ppm (m's, C_6H_4), 1.1−3.2 ppm (m's, cyclohexyl and methylene protons).

Kinetics of CO_2 Reduction. Cyclic voltammetry experiments were used to determine the kinetics of the catalytic reaction. In all cases, 2.0 mL of a 0.3 M solution of Et_4NBF_4 in dimethylformamide was used, and ferrocene was added as an internal reference. The working electrode was a glassy carbon disk, the counter electrode was a glassy carbon rod, and an electrode consisting of a platinum wire inserted into a 1:1 solution (1 mM each) of decamethylferrocene/decamethylferrocenium in acetonitrile was used as a psuedoreference electrode.

Order with Respect to Acid. This was determined by titration with tetrafluoroboric acid. To a dimethylformamide solution was added catalyst to make the solution 2 mM in catalyst. The solution was purged with N_2, and an initial cyclic voltammogram was recorded. After a 15 min CO_2 purge to saturate the solution, aliquots of aqueous 7.6 M HBF_4 solution were added and the cyclic voltammograms were recorded to determine the catalytic currents. A plot of i_c/i_d versus $[H^+]$ was used to determine the order with respect to H^+. The peak current observed under 1 atm of N_2 in the absence of acid is i_d, and the peak or plateau current observed in the presence of various amounts of acid and 620 mmHg of CO_2 is i_c.

Order with Respect to Catalyst. A stock solution of 0.120 M catalyst in DMF containing electrolyte was prepared. Acid was added to the solution in the cell to make it 0.1 M HBF_4, and it was purged with CO_2. Then aliquots of the catalyst solution were added, and cyclic voltammograms were recorded. A plot of peak or plateau current versus the catalyst concentration was used to determine the order.

Order with Respect to CO_2. Acid (0.1 M) and catalyst (2 mM) were added to the electrolyte solution in the cell. The cell was first purged with N_2, then with 3% CO_2, 10% CO_2, 30% CO_2, and pure CO_2, recording cyclic voltammograms after each purge. Concentrations of CO_2 in solution were based on a concentration of 0.18 M for a saturated solution of 100% CO_2 in dimethylformamide at 620 mmHg.[18] A plot of current versus the square root of the CO_2 concentration was used to determine the order of the reation in CO_2.

Catalytic Coulometry. A three-necked flask with a stopcock having a total volume of 120 mL was used for bulk electrolysis experiments. One neck was a 24/40 joint that accepted a stainless steel 24/40 fitting with an insulated copper wire running through it. To this was attached a cylinder of retriculated vitreous carbon as a working electrode. The other two necks of the flask were 14/20 joints. Both were fitted with glass compartments with Vycor frits on the bottom. One was used as the reference electrode; it was filled with a solution of decamethylferrocene/decamethylferrocenium in acetonitrile, and a Pt wire was inserted. The other was used as the counter electrode, and it contained a saturated solution of ferrocene in 0.3 M Et_4NBF_4 in DMF and a tungsten wire. Gas was introduced into the sealed flask through the stopcock. The cell was typically filled with 15 mL of a 0.3 M Et_4NBF_4 solution in dimethylformamide. Acid (0.1 M) and catalyst (1 mM) were added to the solution, which was then purged with CO_2 for 15 min. Controlled potential coulometry was performed in 1 h increments at −1.0 to −1.1 V versus the decamethylferrocene/decamethylfer-

(6) (a) Nagao, H.; Mizukawa, T.; Tanaka, K. *Chem. Lett.* **1993**, 955−958. (b) Summers, D. P.; Frese, K. W., Jr. *J. Electroanal. Chem.* **1986**, *205*, 219−232. (c) Shin, W.; Lee, S. H.; Shin, J. W.; Lee, S. P.; Kim, Y. *J. Am. Chem. Soc.* **2003**, *125*, 14688−14689.

(7) (a) Hori, Y.; Kikuchi, K.; Suzuki, S. *Chem. Lett.* **1985**, 1695−1698. (b) Hori, Y.; Kikuchi, K.; Murata, A.; Suzuki, S. *Chem. Lett.* **1986**, 897−898. (c) Hori, Y.; Murata, A.; Takahashi, R.; Suzuki, S. *J. Chem. Soc., Chem. Commun.* **1988**, 17−19. (d) Hori, Y.; Murata, A.; Takahashi, R. *J. Chem. Soc., Faraday Trans. 1* **1989**, *85*, 2309−2326. (e) Hori, Y.; Takahashi, I.; Koga, O.; Hoshi, N. *J. Mol. Catal. A: Chem.* **2003**, *199*, 39−47. (f) Hoshi, N.; Hori, Y. *Electrochim. Acta* **2000**, *45*, 4263−4270. (g) Hoshi, N.; Sato, E.; Hori, Y. *J. Electroanal. Chem.* **2003**, *540*, 105−110. (h) Frese, K. W., Jr.; Leach, S. *J. Electrochem. Soc.* **1985**, 259−260.

(8) DuBois, D. L. *Comments Inorg. Chem.* **1997**, *19*, 307−325.

(9) DuBois, D. L.; Miedaner, A.; Haltiwanger, R. C. *J. Am. Chem. Soc.* **1991**, *113*, 8753−8764.

(10) Bernatis, P. R.; Miedaner, A.; Haltiwanger, R. C.; DuBois, D. L. *Organometallics* **1994**, *13*, 4835−4843.

(11) Wander, S. A.; Miedaner, A.; Noll, B. C.; Barkley, R. M.; DuBois, D. L. *Organometallics* **1996**, *15*, 3360−3373.

(12) Steffey, B., D.; Curtis, C. J.; DuBois, D. L. *Organometallics* **1995**, *14*, 4937−4943.

(13) Miedaner, A.; Curtis, C. J.; Barkley, R. M.; DuBois, D. L. *Inorg. Chem.* **1994**, *33*, 5482−5490.

(14) (a) Sen, A.; Ta-Wang, L. *J. Am. Chem. Soc.* **1981**, *103*, 4627. (b) Hathaway, B. J.; Holah, D. G.; Underhill, A. E. *J. Chem. Soc.* **1962**, 2444.

(15) Tavs, P. *Chem. Ber.* **1970**, *103*, 2428−2436.

(16) Kyba, E. P.; Liu, S.-T.; Harris, R. L. *Organometallics* **1983**, *2*, 1877−1879.

(17) Askham, F. R.; Stanley, G. C.; Marques, E. C. *J. Am. Chem. Soc.* **1985**, *107*, 7423−7431.

(18) Stephen, H., Stephen, T., Eds. *Solubilities of Inorganic and Organic Compounds*; Pergamon Press: New York, 1958; Vol. 1, p 1063.

Table 1. Crystal and Refinement Data for {*m*-(triphos)$_2$[Pd(CH$_3$CN)]$_2$}(BF$_4$)$_4$, 2

chemical formula	$C_{72.78}H_{124.56}B_4Cl_{1.56}F_{16}N_5P_6Pd_2$
fw	1870.86
space group	$P2_1/n$ (No. 14)
a	21.125(6) Å
b	12.386(3) Å
c	27.917(6) Å
α	90°
β	92.821(5)°
γ	90°
V	8677(3) Å^3
Z	4
color, habit	orange plate
cryst dimens	0.28 × 0.26 × 0.12 mm
temperature	−138(2) °C
λ	0.71073 Å
μ	0.650 mm^{-1}
density (calcd)	1.432 g·cm^{-3}
no. of reflns collected	42 928
no. of indep reflns	11 339 (R(int) = 0.0845)
no. of params	909
R1[a] (F, $I > 2\sigma(I)$)	0.0823
wR2[b] (F^2)	0.2383
goodness of fit[c]	1.056

[a] $R1 = \sum||F_o| - |F_c||/\sum|F_o|$. [b] $wR2 = \{\sum[w(F_o^2 - F_c^2)^2]/\sum[w(F_o^2)^2]\}^{1/2}$, $w^{-1} = [\sigma^2(F_o^2) + (0.1325P)^2 + 9.6648P]$; $P = (F_o^2 + 2F_c^2)/3$. [c] Goof = $S = \{\sum[w(F_o^2 - F_c^2)^2]/(n - p)\}^{1/2}$, n = number of reflections, p = number of parameters.

rocenium reference electrode. Samples of the gas in the headspace of the flask were removed every 20 min via a gastight syringe and analyzed by gas chromatography to determine the amount of H_2 and CO generated. After 15 h, 190 mole of CO were produced per mole of catalyst. A sample of the catalytic solution was analyzed by ^{31}P NMR spectroscopy, and 82% of the original catalyst remained.

Gas Chromatography. GC was performed using a Perkin-Elmer AutoSystem gas chromatograph. Gas samples were collected with a 0.1 mL gas syringe. Chromatograms were obtained and analyzed using Perkin-Elmer Turbochrom Workstation software. The GC was calibrated for H_2 and CO by injecting known quantities of pure gas into the bulk electrolysis cell and then analyzing a 0.1 mL sample of the headspace. A calibration curve was generated for both hydrogen and carbon monoxide.

X-ray Crystallography. Crystals were examined under light hydrocarbon oil. The datum crystal was mounted to the tip of a thin glass fiber affixed to a tapered copper mounting pin and placed into the goniometer of a Siemens SMART CCD diffractometer equipped with an LT-2A low-temperature apparatus operating at 135 K. Cell dimensions were determined after harvesting reflections from three orthogonal sets of 20 0.3° *ω* scans and were refined using 8483 reflections harvested from the entire data collection. An arbitrary hemisphere of data was collected to 0.68 Å resolution using 0.3° *ω* scans, each measured for 30 s. The data were truncated to 0.92 Å during refinement because of weak diffraction and poor agreement between equivalents at higher angles. All data were corrected for Lorentz and polarization effects, as well as for absorption.

Structure solution via direct methods in centrosymmetric space group $P2_1/n$ revealed most of the cation structure and several of the anions. Cycles of least-squares refinement followed by difference Fourier map calculation uncovered the missing atoms and showed disorder in three cyclohexyl groups. In addition, a region of electron density was discovered. This was modeled as three heavily disordered molecules of acetonitrile using the routine SQUEEZE from the package PLATON (Speck, University of Utrecht, 2004). All non-hydrogen atoms were refined using parameters for anisotropic thermal motion. Hydrogens were placed at calculated geometries and allowed to ride on the position of the parent atom. Hydrogen thermal motion was modeled isotropically using U equal to 1.2× the equivalent isotropic U of the parent atom (1.5× for methyl hydrogens). Crystal and refinement data are listed in Table 1.

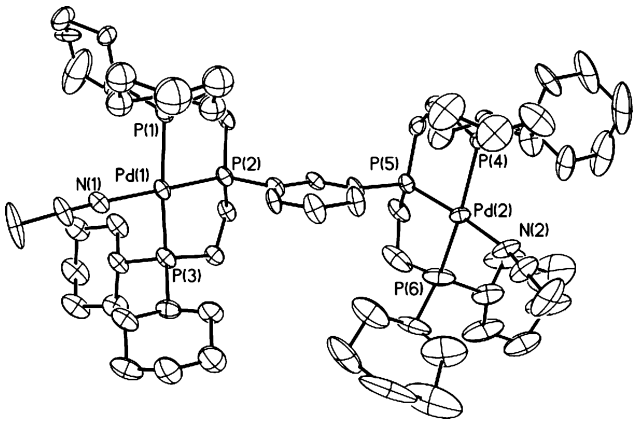

Figure 1. ORTEP drawing of {*m*-(triphos)$_2$[Pd(CH$_3$CN)]$_2$}$^{4+}$ cation showing 30% probability ellipsoids and the atom-numbering scheme.

Results

Catalyst Synthesis and Characterization. The bis(triphosphine) ligand $C_6H_4\{P[CH_2CH_2P(C_6H_{11})_2]_2\}_2$, *m*-(triphos)$_2$ (**1**), can be prepared by the reaction of *m*-bis(phosphino)benzene with 4 equiv of vinyldicyclohexylphosphine using AIBN as a free radical initiator, step 1 of reaction 1. The ^{31}P NMR spectrum of the product consists of a doublet at 1.55 ppm assigned to the terminal dicylohexylphosphine group and a triplet at −14.38 ppm assigned to the central phosphorus atom of the triphosphine moiety. The observed three-bond phosphorus−phosphorus coupling of 25 Hz is typical for triphosphine ligands with two-carbon backbones, and the calculated chemical shifts of 0 and −16 ppm for the terminal and central phosphorus atoms are in good agreement with the experimental values (1.55 and −14.38 ppm, respectively).[9,19]

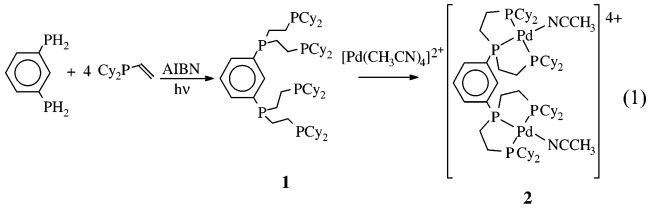

(1)

Reaction of **1** with $[Pd(CH_3CN)_4]^{2+}$ results in the formation of {*m*-(triphos)$_2$[Pd(CH$_3$CN)]$_2$}$^{4+}$ (**2**), step 2 of reaction 1. The ^{31}P NMR spectrum of **2** consists of a triplet at 119.4 ppm ($^3J_{PP}$ = 4 Hz) and a doublet at 76.6 ppm assigned to the central and terminal phosphorus atoms, respectively. These chemical shifts and the coupling constant are very similar to those of monomeric $[Pd(etpC)(CH_3CN)]^{2+}$ [115.6 ppm (central P), 74.5 ppm (terminal P), and 7 Hz; where etpC is bis(dicyclohexylphosphinoethyl)phenylphosphine)].[9] ^{1}H NMR spectral data and elemental analysis are also consistent with the formulation shown for **2** (see Experimental Section).

An X-ray diffraction study confirms the structure proposed for **2**, although there is disorder in the cyclohexyl rings, anions, and solvent molecules. The crystals of **2**(BF$_4$)$_4$ consist of {*m*-triphos[Pd(CH$_3$CN)]$_2$}$^{4+}$ cations, BF_4^- anions, and solvent

(19) Steffey, B. D.; Miedaner, A.; Maciejewski-Farmer, M. L.; Bernatis, P. R.; Herring, A. M.; Allured, V. S.; Carperos, V.; DuBois, D. L. *Organometallics* **1994**, *13*, 4844−4855.

Table 2. Selected Bond Lengths and Bond Angles for $\{m\text{-(triphos)}_2[Pd(CH_3CN)]_2\}^{4+}$ (2) and $[Pd(MesetpE)(CH_3CN)]^{2+}$

$\{m\text{-(triphos)}_2[Pd(CH_3CN)]_2\}^{4+}$				$[Pd(MesetpE)(CH_3CN)]^{2+}$	
Pd(1)(P1)(P2)(P3)(N1)		Pd(2)(P4)(P5)(P6)(N2)			
Bond Lengths (Å)					
Pd(1)−P(1)	2.342(3)	Pd(2)−P(4)	2.337(3)	Pd(1)−P(1)	2.324
Pd(1)−P(2)	2.211(3)	Pd(2)−P(5)	2.204(3)	Pd(1)−P(2)	2.231
Pd(1)−P(3)	2.326(3)	Pd(2)−P(6)	2.332(3)	Pd(1)−P(3)	2.338
Pd(1)−N(1)	2.070(9)	Pd(2)−N(2)	2.059(10)	Pd(1)−N(1)	2.057
C(30)−N(1)	1.132(12)	C(15)−N(2)	1.118(14)	C(22)−N(1)	1.119
Bond Angles (deg)					
P(1)−Pd(1)−P(2)	84.66(10)	P(4)−Pd(2)−P(5)	83.57(10)	P(1)−Pd(1)−P(2)	84.9
P(1)−Pd(1)−P(3)	166.02(10)	P(4)−Pd(2)−P(6)	162.32(11)	P(1)−Pd(1)−P(3)	164.9
P(1)−Pd(1)−N(1)	95.8(2)	P(4)−Pd(2)−N(2)	98.2(3)	P(1)−Pd(1)−N(1)	95.0
P(2)−Pd(1)−P(3)	84.60(10)	P(5)−Pd(2)−P(6)	83.37(13)	P(2)−Pd(1)−P(3)	84.2
P(2)−Pd(1)−(N1)	177.1(2)	P(5)−Pd(2)−(N2)	172.6(3)	P(2)−Pd(1)−(N1)	176.6
P(3)−Pd(1)−(N1)	94.5(2)	P(6)−Pd(2)−(N2)	96.3(3)	P(3)−Pd(1)−(N1)	95.1

molecules. A drawing of the cation is shown in Figure 1, and Table 2 lists selected bond distances and angles of the cation. The drawing illustrates the square-planar structure of the two $[Pd(triphosphine)(CH_3CN)]^{2+}$ units. These two units rotate about the two P−C bonds attaching them to the benzene ring (C33−P5 and C31−P2) so that unfavorable steric interactions are avoided. The observed Pd−P and Pd−N bond distances and the bond angles within the first coordination sphere are very similar to those observed previously for $[Pd(MesetpE)(CH_3CN)]^{2+}$ (where MesetpE is bis(2-diethylphosphinoethyl)-mesitylphosphine)), which are shown in Table 2 for comparison.[10] The P−Pd−P bond angles associated with the five-membered rings are all acute (83−85°). These acute angles are caused by the restricted bite size of the triphosphine ligands. The $N-Pd-P_{cis}$ angles are all greater than 90° to compensate for acute P−Pd−P angles of the triphosphine ligand. The Pd−P bond distances for the central phophorus atoms are at least 0.1 Å shorter than the Pd−P bond distances to the terminal phosphorus atoms. The most likely cause of this difference is the stronger trans influence of phosphorus compared to nitrogen, but restricted vibrational amplitudes arising from incorporation into two rings may also contribute to the observed difference.

Catalytic Studies. Cyclic voltammograms recorded on complex **2** in dimethylformamide under four different conditions are shown in Figures 2 and 3. The black trace in Figure 2 is the cyclic voltammogram of **2** under a nitrogen atmosphere. It exhibits a broad irreversible cathodic wave at −1.38 V versus the ferrocene/ferrocenium couple. If this solution is saturated with CO_2 at 1 atm pressure, the cyclic voltammogram shown by the red trace in Figure 2 is obtained. Under CO_2 three irreversible waves are observed at −1.41, −1.51, and −1.75 V. The first two of these are strongly overlapping, which leads to a single broad wave with two humps. At all potentials more negative than the onset potential of the first reduction wave, the current is higher in the presence of CO_2 than in the absence of CO_2. This suggests that catalysis is occurring even in the absence of an added proton source. Presumably CO_2 acts as an acceptor for O^{2-} to form carbonate. In the presence of both HBF_4 and CO_2, the green trace in Figure 3, a large catalytic wave is observed for the reduction of CO_2. In the presence of HBF_4 but no CO_2, the blue trace in Figure 3 is obtained. In this case a broad, poorly defined reduction wave is observed that corresponds to the catalytic reduction of protons to H_2. These cyclic voltammetry results suggest, but do not prove, that **2** is a catalyst for CO_2 reduction. For example, cyclic voltammograms of the complex $[Pd(PCP)(CH_3CN)]^+$ [where PCP is 2,6-bis(diphenylphosphinomethyl)phenyl] also show enhanced current in the presence of CO_2, but the product formed in the presence of acid and CO_2 is hydrogen and not CO. For $[Pd(PCP)(CH_3CN)]^+$, CO_2 acts as a cocatalyst for hydrogen generation.[19]

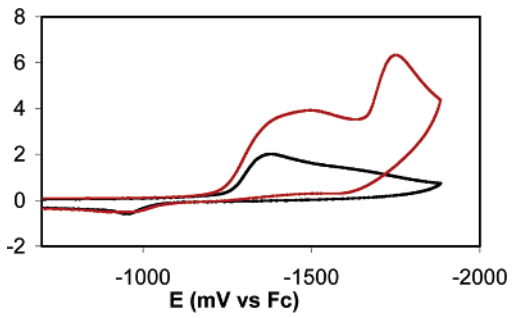

Figure 2. Cyclic voltammograms of 2 mM **2** under an atmosphere of N_2 (black trace) and under an atmosphere of CO_2 (0.18 M, red trace).

Catalytic reduction of CO_2 by **2** was confirmed by carrying out controlled-potential electrolyis experiments on the plateau of the catalytic wave (−1.7 V) for dimethylformamide solutions containing 0.1 M HBF_4 and a large headspace of CO_2 at 620 mmHg (see Experimental Section). The current efficiencies for CO and H_2 production were determined to be 80% and 26%, respectively, by gas chromatography. Because this experiment and previous experiments for this class of catalysts were conducted in dimethylformamide, the formation of trace amounts of formate would be obscured by formate formation from solvent decomposition. After a total of 190 turnovers of the catalyst for CO production, a ^{31}P NMR analysis of the solution indicated that 82% of the catalyst was unchanged.

Kinetic Studies. For a reversible electron-transfer reaction followed by a fast catalytic reaction at high substrate concentrations, the ratio between the catalytic current, i_c, and the diffusion

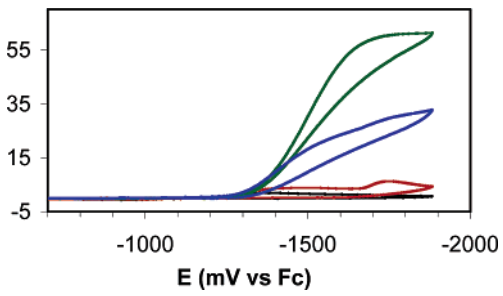

Figure 3. Cyclic voltammograms of 2 mM **2** under an atmosphere of N_2 (black trace), under an atmosphere of CO_2 (0.18 M, red trace), in the presence of both 0.18 M CO_2 and 0.1 M acid (green trace), and in the presence of 0.1 M acid under nitrogen (blue trace).

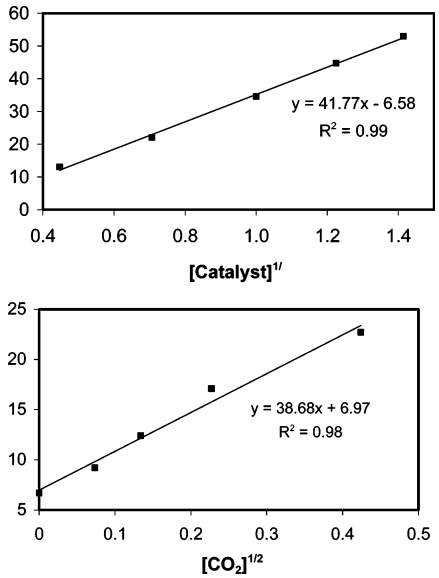

Figure 4. Plots of i_c versus $[CO_2]^{1/2}$ (bottom graph) and versus $[Cat]^{1/2}$ (top graph) under conditions described in the Experimental Section. Concentration units are $M^{1/2}$ for the bottom graph and $mM^{1/2}$ for the top graph.

current observed for the reduction of the catalyst in the absence of substrates, i_d, is given by eq 2.[20]

$$\frac{i_c}{i_d} = \frac{\sigma}{0.447}\sqrt{\frac{RT}{nF}}\sqrt{\frac{kC^m}{\nu}} \qquad (2)$$

where n is the number of electrons involved in catalyst reduction (2 in this case), k is the rate constant, ν is the scan rate, C is the concentration of the substrate (CO_2), and m is an exponent corresponding to the reaction order of the substrate. The value of the factor designated by σ in eq 2 depends on whether the second electron transfer to the catalyst occurs in solution or at the electrode surface. If the second electron transfer occurs in solution—a SET mechanism—the value of σ is $2^{1/2}$. If the second electron transfer occurs at the electrode surface—an ECE mechanism—the value of σ is 2. In previous work, a value of 2 was used for this parameter, and this value is used in this study as well. From eq 2 it can be seen that a plot of the catalytic current versus the square root of the CO_2 concentration should be linear if the reaction is first order in CO_2. Such a plot is shown in the bottom graph of Figure 4. The catalytic current also shows a square root dependence on the catalyst concentration, top graph of Figure 4. In the case of the catalyst, the current shows a first-order dependence if the reaction is first order in catalyst, a second-order dependence if the reaction is second order, etc.[20] Therefore a square root dependence on catalyst concentration indicates that only half of the bimetallic complex is required for catalysis. The transition state of a given catalytic cycle contains one palladium center and one CO_2. This indicates that the two palladium atoms act independently of each other.

The dependence of the catalytic current on acid is shown by the red circles in Figure 5. These data are uncorrected for any background current that may be due to hydrogen production. The blue circles indicate data in which the current in the absence of CO_2, i.e., the current observed at different acid concentrations, is subtracted. Both of these data sets indicate that at low acid concentrations the current exhibits a strong dependence on the acid concentration, but at higher acid concentrations the current approaches a limiting value that is independent of the acid concentration. This behavior indicates the presence of two rate-determining steps depending on the reaction conditions.

In previous work on monomeric $[Pd(triphosphine)(CH_3CN)]^{2+}$ catalysts, eq 2 was modified to eq 3 to account for this behavior.[9,10] In this equation, both the acid and CO_2

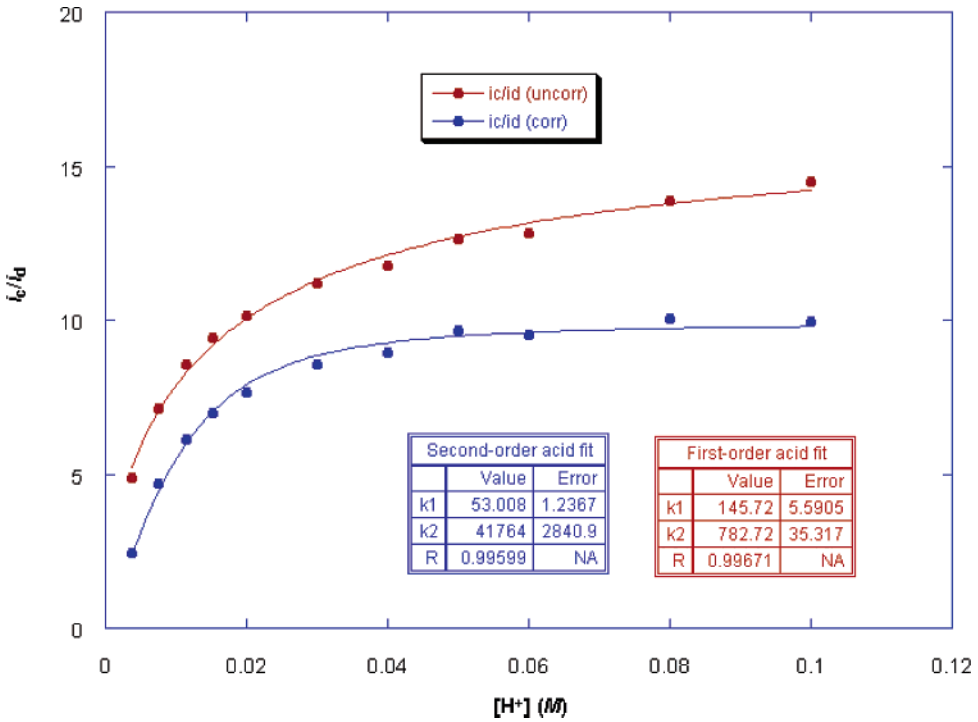

Figure 5. Plots of the ratio of the catalytic current (i_c) to the diffusion current (i_d) as a function of the acid concentration for a dimethylformamide solution containing 2 mM **2** and 0.18 M CO_2. The red circles are uncorrected for current observed in the absence of CO_2. The blue circles are corrected by subtracting the current observed in the absence of CO_2 from current in the presence of CO_2. The solid circles represent data points; the lines represent the best least-squares fits of the data to eq 3 assuming first-order dependence on acid (red) and second-order dependence on acid (blue).

concentrations are treated explicitly, and k_1 is the second-order rate constant for the reaction of CO_2 with the Pd(I) species formed on reduction of Pd(II). The rate constant k_2 is a composite constant and not a simple rate constant. It can be seen that depending on whether a background correction is made, the data can be fitted for either a first-order (red curve) or second-order (blue curve) acid dependence. Because of this, the correct order of the catalytic reaction with respect to the acid concentration is ambiguous, and two different rate constants for k_1 are obtained, 145 M^{-1} s^{-1} assuming a first-order dependence on $[H^+]$ and 53 M^{-1} s^{-1} assuming a second-order dependence on $[H^+]$. However, there is no doubt that there is an acid dependence.

$$\frac{i_c}{i_d} = \frac{\sigma}{0.447}\sqrt{\frac{RT}{nF\nu}}\sqrt{\frac{k_1 k_2[CO_2][H^+]^m}{k_1[CO_2] + k_2[H^+]^m}} \qquad (3)$$

Discussion

In previous work, we have described the electrocatalytic reduction of CO_2 by monometallic $[Pd(triphosphine)(CH_3CN)]^{2+}$ complexes (**3**), the bimetallic complex $[Pd_2(CH_3CN)_2(eHTP)]^{4+}$ (**4**), and dendrimers **5** and **6**. The monometallic complexes **3** are excellent catalysts for the reduction of CO_2 to CO. The rate-limiting step in the catalytic cycle for these complexes is the reaction of the reduced Pd(I) catalyst with CO_2. Second-order rate constants for this reaction range from 5 to 300 M^{-1} s^{-1}, making these catalysts some of fastest CO_2 reduction catalysts known.[8−11] They also operate at moderate overpotentials and can exhibit current efficiencies for CO production exceeding 90%. However, measured turnover numbers are less than 150. It was found that one of the major decomposition pathways for these monometallic palladium complexes was the formation of bimetallic Pd(I) dimers having structure **7**.[9] This decomposition pathway is retarded by the use of bulky substituents such as cyclohexyl groups on the terminal phosphorus atoms, but deactivation still occurs. One attempt to increase the stability of these complexes was to incorporate them into dendrimers such as **5** and **6**.[13] The premise underlying the study of these

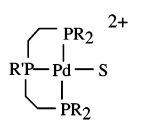

3

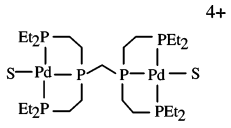

4

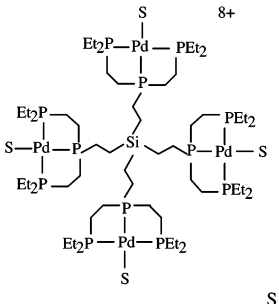

5

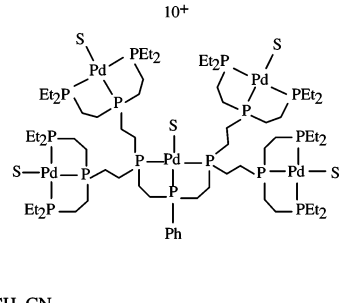

6

S = CH_3CN

dendrimers was that the restricted positions of the $[Pd(triphosphine)(CH_3CN)]^{2+}$ units within the dendrimers would prevent Pd−Pd bond formation. However, the selectivity of these dendrimers for CO production was decreased and the turnover numbers were generally less than those of their monometallic analogues, **3**. It was concluded from these studies that increased turnover numbers for dendrimers might be possible if the $[Pd(triphosphine)(CH_3CN)]^{2+}$ units were more isolated from each other.

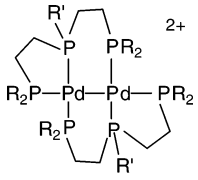

7

A second reason for interest in dendrimers **5** and **6** was the possibility of cooperative interactions between metal sites during CO_2 reduction. There is considerable literature precedent that CO_2 binding can be stabilized by the interaction of two metals.[21] In these systems one metal binds to a carbon atom and the second metal binds to oxygen. However, no evidence of cooperative interaction between the palladium atoms was observed for dendrimers **5** and **6**. In contrast, kinetic studies of the bimetallic complex **4** indicated that the transition state formed by the reaction of the Pd(I) form of **4** with CO_2 involved both metal atoms and one proton.[19] This is consistent with a cooperative interaction between metals for CO_2 reduction, and the rate constant appeared to be significantly higher (10^4 M^{-1} s^{-1}). However, decomposition of this Pd(I) intermediate was also much faster and a turnover number of 8 was observed for **4**.

The dipalladium complex **2** was prepared to determine if beneficial cooperative effects observed for **4** would be preserved if the distance between the central phosphorus atoms of the two triphosphine units was increased. A second objective was to determine if catalyst degradation could be retarded by incorporating cyclohexyl substituents on the terminal phosphorus atoms and increasing the intramolecular Pd−Pd distance relative to **4**. The kinetic results described above for **2** demonstrate that the transition state that occurs during the catalytic reduction of CO_2 to CO involves only one palladium atom, one CO_2 molecule, and one or two protons. These results indicate that the cooperative interaction between two palladium atoms observed for complex **4** is not observed for **2** and that the two $[Pd(triphosphine)(CH_3CN)]^{2+}$ units act independently during the catalytic process. The catalytic rates of **2** (50−150 M^{-1} s^{-1}) and its analogous monomeric complex $[Pd(etpC)(CH_3CN)]^{2+}$ (50 M^{-1} s^{-1}) are also quite comparable. This also suggests that no cooperative interaction between the two palladium atoms occurs during the catalytic cycle of **2**. Cooperative binding of CO_2 for **2** is apparently prevented by the bulkiness of the cyclohexyl substituents. However, the stability of **2** is greater than its monometalic analogue, $[Pd(etpC)(CH_3CN)]^{2+}$, and complexes **4**−**6**. Complex **2** undergoes less than 20% degradation after nearly 200 turnovers. Previous turnover numbers of 130, 8, 15, and 5 for $[Pd(etpC)(CH_3CN)]^{2+}$, **4**, **5**, and **6**, respectively, were determined when 10% or less of the original catalytic activity remained. Retention of 80% of **2** after nearly 200 turnovers indicates that the turnover numbers for this complex are at least 1−2 orders of magnitude greater than for

(20) (a) Savéant, J.-M.; Vianello, E. *Electrochim. Acta* **1965**, *10*, 905. (b) Hammouche, M.; Lexa, D.; Momenteau, M.; Savéant, J.-M. *J. Am. Chem. Soc.* **1991**, *113*, 8455.

(21) (a) Gibson, D. H. *Chem. Rev.* **1996**, *96*, 2063. (b) De Angelis, S.; Solari, E.; Gallo, E.; Floriani, C.; Chiesi-Villa, A.; Rizzoli, C. *Inorg. Chem.* **1996**, *35*, 5995. (c) Schmidt, M. H.; Miskelly, G. M.; Lewis, N. S. *J. Am. Chem. Soc.* **1990**, *112*, 3420−3426.

$[Pd(etpC)(CH_3CN)]^{2+}$ and **4**−**6**. The increased stability of **2** is attributed to a combination of the steric interactions of the cyclohexyl groups and an intramolecular restriction of the Pd−Pd distance in **2** that arises from the constraints of the *m*-benzene bridge. Both of these features should retard Pd−Pd bond formation.

In summary, the new bimetallic palladium complex **2** has been prepared and characterized by NMR spectroscopy and an X-ray diffraction study. Complex **2** is a catalyst for the electrochemical reduction of CO_2 to CO. Kinetic studies indicate that the transition state involves one palladium, one CO_2 molecule, and either one or two protons. Therefore the two palladium atoms of **2** act independently of each other during the catalytic cycle. However, because of the steric constraints of the cyclohexyl substituents and the brindging *m*-benzene backbone, **2** exhibits significantly higher turnover numbers than other members of this class of catalysts.

Acknowledgment. The support of the Director's Discretionary Research and Development Program of the National Renewable Energy Laboratory is gratefully acknowledged.

Supporting Information Available: X-ray structural data including tables of crystal and refinement data, atomic positional and thermal parameters, and interatomic distances and angles for $\{m\text{-(triphos)}_2[Pd(CH_3CN)]_2\}(BF_4)_4$ (CIF). This material is available free of charge via the Internet at http://pubs.acs.org.

OM060228G